Accepted Manuscript

Gut-specific Delivery of T-helper 17 Cells Reduces Obesity and Insulin Resistance in Mice

Chun-Pyo Hong, Areum Park, Bo-Gie Yang, Chang Ho Yun, Min-Jung Kwak, Gil-Woo Lee, Jung-Hwan Kim, Min Seong Jang, Eun-Jung Lee, Eun-Ji Jeun, Gihoon You, Kwang Soon Kim, Youngwoo Choi, Ji-Hwan Park, Daehee Hwang, Sin-Hyeog Im, Jihyun F. Kim, Yoon-Keun Kim, Ju-Young Seoh, Charles D. Surh, You-Me Kim, Myoung Ho Jang

PII: S0016-5085(17)30180-4
DOI: 10.1053/j.gastro.2017.02.016
Reference: YGAST 60999

To appear in: *Gastroenterology*
Accepted Date: 20 February 2017

Please cite this article as: Hong C-P, Park A, Yang B-G, Yun CH, Kwak M-J, Lee G-W, Kim J-H, Jang MS, Lee E-J, Jeun E-J, You G, Kim KS, Choi Y, Park J-H, Hwang D, Im S-H, Kim JF, Kim Y-K, Seoh J-Y, Surh CD, Kim Y-M, Jang MH, Gut-specific Delivery of T-helper 17 Cells Reduces Obesity and Insulin Resistance in Mice, *Gastroenterology* (2017), doi: 10.1053/j.gastro.2017.02.016.

Gut-specific Delivery of T-helper 17 Cells Reduces Obesity and Insulin Resistance in Mice

Short Title: Gut-Specific T_H17 Cells Control Obesity

Authors

Chun-Pyo Hong[1,2,3], Areum Park[2], Bo-Gie Yang[1], Chang Ho Yun[1], Min-Jung Kwak[4,5], Gil-Woo Lee[1,2], Jung-Hwan Kim[1,2], Min Seong Jang[1,2], Eun-Jung Lee[1,2], Eun-Ji Jeun[1,2], Gihoon You[2], Kwang Soon Kim[1], Youngwoo Choi[6], Ji-Hwan Park[7], Daehee Hwang[7,8], Sin-Hyeog Im[1,2], Jihyun F. Kim[4], Yoon-Keun Kim[9], Ju-Young Seoh[3], Charles D. Surh[1,2], You-Me Kim[2,6,*] and Myoung Ho Jang[1,10,*]

[1]Academy of Immunology and Microbiology, Institute for Basic Science, Pohang 37673, Republic of Korea

[2]Division of Integrative Biosciences and Biotechnology, Pohang University of Science and Technology, Pohang 37673, Republic of Korea

[3]Department of Microbiology, Graduate School of Medicine, Ewha Womans University, Seoul 07985, Republic of Korea

[4]Department of Systems Biology and Division of Life Sciences, Yonsei University, Seoul 03922, Republic of Korea

[5]Biosystems and Bioengineering Program, Korea University of Science and Technology, Daejeon 34113, Republic of Korea

[6]Department of Life Science, Pohang University of Science and Technology, Pohang 37673, Republic of Korea

[7]Department of Chemical Engineering, Pohang University of Science and Technology, Pohang 37673, Republic of Korea

[8]Center for Plant Aging Research, Institute for Basic Science, Daegu 42988, Republic of Korea

[9]Research Institute, MD Healthcare, Seoul 03923, Republic of Korea

[10]WPI Immunology Frontier Research Center, Osaka University, Suita 565-0871, Japan

Authorship note: Chun-Pyo Hong, Areum Park and Bo-Gie Yang contributed equally to this work.

Acknowledgements

We thank Jin-Myung Bae for excellent technical assistance, Kwan Seok Lee for mouse husbandry, Hae Jin Jung for assistance with cell sorting, Seung-Woo Lee for helpful discussion, and Wonhwa Cho for careful reading of the manuscript. This work was supported by grants from Institute for Basic Science (IBS-R005-S1-2015-a00 and IBS-R005-D1-2015-a00), National Research Foundation (NRF-2011-0017670, NRF-2014M3C9A3068822, NRF-2015R1A2A2A04003471, NRF-2016R1A2B3015046) of the Ministry of Science, ICT and Future Planning, BK21 Plus (10Z20130012243), and POSCO (2015Y060).

Abbreviations used in this paper: HFD, high fat diet; SP, spleen; MLN, mesenteric lymph nodes; VAT, visceral adipose tissue; GF, germ-free; SPF, specific pathogen-free; SFB, segmented filamentous bacteria; SI, small intestine; LP, lamina propria; NCD, normal chow diet; VAD, vitamin A-depleted HFD; VAS, vitamin A-sufficient HFD; RA, retinoic acid; UEA-1, Ulex europaeus agglutinin 1; IFN-γ, interferon- γ; DCs, dendritic cells.

*Correspondence should be addressed to:

Myoung Ho Jang

WPI Immunology Frontier Research Center, Osaka University

Mailing address: IFReC Research Building, Osaka University, 3-1 Yamadaoka, Suita, 565-0871, Osaka, Japan

Phone: +81-6-6879-8333

FAX: +81-6-6879-8332

E-mail address: jang@ifrec.osaka-u.ac.jp

You-Me Kim

Division of Integrative Biosciences and Biotechnology

Pohang University of Science and Technology

Mailing address: Pohang University of Science and Technology, POSTECH Biotech Center 270, 77 Cheongam-ro, Nam-gu, Pohang, 37673, Republic of Korea

Phone: +82-54-279-0689

FAX: +82-54-279-0898

E-mail address: youmekim@postech.ac.kr

Conflict of interest statement

The authors have declared that no conflict of interest exists.

Author contributions

C.-P.H., A.P., B.-G.Y., Y.-M.K., and M.H.J. designed experiments, interpreted data, and wrote the paper.

S.-H.I, J.-Y.S, and C.D.S designed experiments and interpreted data.

C.-P.H., A.P., B.-G.Y., C.H.Y., G.-W.L., J.-H.K., M.S.J., E.-J.L., E.-J.J., G.Y., and K.S.K. performed experiments.

M.-J.K., Y.C., J.F.K., and Y.-K.K. performed metagenomic analysis of gut microbiota.

J.-H.P and D.H performed analysis of T_H17 cells.

ABSTRACT

Background & Aims: Obesity and metabolic syndrome have been associated with alterations to the intestinal microbiota. However, few studies examined the effects of obesity on the intestinal immune system. We investigated changes in subsets of intestinal CD4+ T-helper (Th) cells with obesity and the effects of gut-tropic Th17 cells in mice on a high-fat diet (HFD).

Methods: We isolated immune cells from small intestine and adipose tissue of C57BL/6 mice fed a normal chow diet or a HFD for 10 weeks and analyzed the cells by flow cytometry. Mice fed a vitamin A-deficient HFD were compared with mice fed a vitamin A-sufficient HFD. Obese RAG1-deficient mice were given injections of only T regulatory cells or a combination of T regulatory cells and Th17 cells (wild type or deficient in integrin β7 subunit-deficient or interleukin 17 [IL17]). Mice were examined for weight gain, fat mass, fatty liver, glucose tolerance, and insulin resistance. Fecal samples were collected before and after T-cell transfer and analyzed for microbiota composition by metagenomic DNA sequencing and quantitative PCR.

Results: Mice placed on a HFD became obese, which affected the distribution of small intestinal CD4+ TH cells. Intestinal tissues from obese mice had significant reductions in the proportion of Th17 cells but increased proportion of Th1 cells, compared with intestinal tissues from non-obese mice. Depletion of vitamin A in obese mice further reduced the proportion of Th17 cells in small intestine; this reduction correlated with more weight gain and worsening of glucose intolerance and insulin resistance. Adoptive transfer of in vitro-differentiated gut-tropic Th17 cells to obese mice reduced these metabolic defects, which required the integrin β7 subunit and IL17. Delivery of Th17 cells to intestines of mice led to expansion of commensal microbes associated with leanness.

Conclusions: In mice, intestinal Th17 cells contribute to development of a microbiota that maintains metabolic homeostasis, via IL17. Gut-homing Th17 cells might be used to reduce metabolic disorders in obese individuals.

KEY WORDS: glucose tolerance; mucosal immunity; intestinal microbiota

The immune system not only defends the host from infection, but also senses the metabolic state and controls metabolic homeostasis.[1-3] Chronic inflammation in metabolic tissues contributes to systemic insulin resistance, and the excessive infiltration and dysregulation of immune cells in visceral adipose tissue (VAT) is a hallmark of obesity-associated metabolic disorders.[3-6] T cells and macrophages infiltrating into VAT produce pro-inflammatory cytokines and reduce insulin sensitivity.[7] In addition, diet-induced obesity contributes to the conversion of M2 macrophages to M1 macrophages, which are important mediators of inflammation.[8] Thus, obesity-induced inflammatory changes are a key pathological factor in metabolic disorders.

Obesity is caused by excessive nutrient absorption in the gut, the organ with the largest number of immune cells. Obesity weakens barrier function of intestinal epithelial cells by reducing mucus-secreting goblet cells[9] and impairing production of antimicrobial peptides from Paneth cells.[10] Moreover, recent evidence links the development of obesity and metabolic syndrome with the disturbance of gut microbiota.[11-13] Alteration of the microbial composition in response to a high fat diet (HFD) causes changes in metabolism and energy harvest.[12] HFD-fed mice show a significant increase in the proportion of *Firmicutes*, along with striking decrease in the proportion of *Bacteroidetes*.[14] In addition, germ-free (GF) mice show resistance to obesity and an altered cholesterol metabolism compared to specific pathogen-free (SPF) mice.[15] Furthermore, microbial transplantation into GF mice from obese mice, compared to lean mice, induces an increase in the fat mass, demonstrating that changes in commensal microbiota can cause the metabolic disorders.[16]

Commensal bacteria can influence the differentiation of T helper cells in the intestine. For instance, several *Clostridium* species and *Bacteroides fragilis* are shown to induce expansion of intestinal regulatory T (Treg) cells while segmented filamentous bacteria (SFB) increases T-helper (T_H) 17 cells.[17] Although the influence of commensal bacteria on

the intestinal immune system and the relationship between obesity and the gut microbiota have been extensively studied, the direct interplay between obesity and the intestinal immune system has not been fully investigated.[18-20]

In this study, we examined changes of intestinal immune cells in HFD-fed obese mice and revealed reciprocal relationship between the intestinal immune system and obesity-induced metabolic syndrome. We found that HFD greatly impacted small intestinal immune cells and led to the pronounced reduction of T_H17 cells. In addition, we found that co-transfer of gut-tropic T_H17 cells along with Treg cells dramatically changed gut microbiota and attenuated obesity and metabolic disorders, indicating that intestinal T_H17 cells play an important role in keeping the metabolic homeostasis. Based on these results, we propose that enhancement of gut-homing T_H17 cells can improve metabolic dysfunction and represents a potential therapeutic strategy.

Materials and Methods

Mice

C57BL/6 (B6), forkhead box P3 (Foxp3)-GFP (B6.Cg-*Foxp3*^{tm2Tch}/J), Rag1-null (B6.129S7-*Rag1*^{tm1Mom}/J), CX3CR1-GFP (B6.129P-*Cx3cr1*^{tm1litt}/J), OT-II (B6.Cg-Tg(TcraTcrb)425Cbn/J), B6/Thy1.1 (B6.PL-*Thy1*^{a}/CyJ), CD45.1 (B6.SJL-*Ptprc*^{a} *Pepc*^{b}/BoyJ**)**, β7 integrin-deficient (B6.Itgb7^{tm1cgn}/J) mice were purchased from the Jackson Laboratory and bred in a specific pathogen-free facility at Pohang University of Science and Technology. Mice in different experimental groups were housed separately. All animal experiments were approved by the Ethics Review Committee for Animal Experimentation of Pohang University of Science and Technology.

Flow cytometry

Cells were stained with fluorescence-conjugated antibodies from BD Biosciences, eBioscience or Biolegend (Supplementary Table 1) after Fc receptor blocking with anti-CD16/CD32 antibody. For intracellular transcription factor staining, Foxp3/Transcription factor staining buffer set (eBioscience) was used. For intracellular cytokine staining, cells were stimulated with phorbol 12-myristate 13-acetate (PMA; 50 ng/ml; Sigma-Aldrich) and ionomycin (750 ng/ml; Sigma-Aldrich) in the presence of monensin (BD GolgiStop^{TM}) for 4h, and stained using Cytofix/Cytoperm staining kit (BD Biosciences). Data were acquired with LSRFortessa (BD Biosciences) or Gallios (Beckman Coulter) and analyzed with FlowJo software (Tree Star).

Diet-induced obesity and metabolic studies

For obesity induction, 6-week-old male mice were fed HFD (60 kcal% fat, Research Diets) for 10 weeks. Control mice were fed with NCD. For vitamin A depletion experiments, mice

were fed a vitamin A-deficient HFD (60% kcal fat without vitamin A, Research Diets) or a vitamin A-sufficient HFD (60% kcal fat with 40,000 IU/kg vitamin A, Research Diets) for 10 weeks. Fasting blood glucose and insulin concentrations were respectively measured by a glucometer (Accu-Chek Performa kit, Roche) and insulin ELISA (Mercodia). For glucose tolerance tests, glucose (2 g/kg body weight) was injected *i.p.* to 16-h-fasted mice and blood glucose levels were measured at indicated time points. For insulin tolerance tests, human insulin (0.75 U/kg body weight) was administered *i.p.* to 4 h-fasted-mice and blood glucose levels were measured at indicated time points.

Isolation of immune cells

Immune cells from the entire small intestine and epididymal adipose tissues were isolated as previously described.[21, 22]

In vitro T cell differentiation

For preparation of T_H17 and T_H1 cells used in the adoptive transfer experiments, naïve T cells ($CD4^+CD44^{lo}CD62L^{hi}CD25^-$) from the spleen and lymph nodes were stimulated with immobilized anti-CD3ε (5 μg/ml, 145-2C11, BD Biosciences) and soluble anti-CD28 (2 μg/ml, 37.51, BD Biosciences) antibodies in the presence of all-*trans* retinoic acid (RA) (1 nM, Sigma Aldrich) for 3-4 days. For T_H17 cell differentiation, the media was supplemented with human transforming growth factor (TGF)-β (5 ng/ml, R&D systems), mouse interleukin (IL)-6 (20 ng/ml, R&D systems), anti-IL-4 (5 μg/ml, 11B11, eBioscience), anti-IL-2 (2.5 μg/ml, S4B6, BD Biosciences) and anti-interferon (IFN)-γ (5 μg/ml, XMG1.2, eBioscience) antibodies. For T_H1 cell differentiation, the media was supplemented with IL-12 (10 ng/ml, R&D systems), IL-2 (20 ng/ml, R&D systems) and anti-IL-4 antibody (5 μg/ml, 11B11,

eBioscience).

Adoptive T cell transfer

T_H1 and T_H17 cells were differentiated *in vitro* as described above. Treg cells ($CD4^+Foxp3\text{-}GFP^+$) were purified from Foxp3-GFP mice. Cells were resuspended in PBS and injected *i.p.* into Rag1-null mice fed HFD for 10 weeks. Recipients were injected with $5x10^5$ Treg alone, the combination of $5x10^5$ Treg and $5x10^5$ T_H1, or the combination of $5x10^5$ Treg and $5x10^5$ T_H17 cells. After the T cell transfer, mice were maintained on HFD for additional 5 weeks, and weight changes, food intake and metabolic parameters were monitored.

Metagenome sequencing and data analysis

Stool samples were collected from the Rag1-null recipient mice (four mice in a single cage for each group) one day before and five weeks after the injection of Treg or Treg/T_H17 cells. Metagenomic DNA was isolated using a stool genomic DNA extraction kit (BIONEER, Korea), and the 16S rRNA genes were amplified with the 27F (5'-AGAGTTTGATCMTGGCTCAG-3') and 518R (5'-GTATTACCGCGGCTGCTG G-3') universal primer set for bacteria and sequenced with 454 GS FLX Titanium (Roche). Read trimming was conducted with CLC Genomics Workbench (ver. 5.1) with quality score set at 0.01, no ambiguous nucleotides, and the minimum read length of 250. After quality trimming, reads containing homo-polymer errors were removed using CD-HIT-OUT and contamination of human DNA was checked with BMTagger program. Taxonomic assignment was performed with high quality reads using RDP-classifier and taxonomic profiling was conducted by comparing relative abundance (confidence value $\geq$ 0.8). Diversity indices, rarefaction curves, and Good's coverages were calculated using mothur. For the principal

coordinate analysis (PCoA), a distance matrix among the groups was constructed using mothur, a neighbor-joining tree was generated using NJdist in ARB software, and the values of PCoA were calculated using UniFrac program.

Quantitative real time PCR

Total RNA was extracted with TRizole reagent (Life Technologies) and cDNA was synthesized using GoScript Reverse Trascription System (Promega). For analysis of relative abundance of specific fecal bacteria, DNA was extracted from feces of mouse using the QIAamp DNA Stool Mini Kit (Qiagen). Quantitative real time PCRs were performed with the primers in Supplementary Table 2 using SYBR Premix Ex Taq (Takara) and Viia 7 real-time PCR instrument (Applied Biosystems).

Histology

Frozen sections of the liver were stained with Oil red O (Sigma Aldrich). Paraffin sections were deparaffinized in xylene, and rehydrated with ethanol. VAT and colon sections were stained with hematoxylin and eosin. Small intestine sections were stained with rhodamine-conjugated *Ulex Europaeus* agglutinin 1 (UEA-1) (20 μg/ml, Vector Laboratories) and mounted in ProLong Gold antifade reagent with DAPI (Life Technologies). The stained sections were imaged using an Olympus FV1000 or ZEIZZ LSM700 confocal microscope.

May-Grunwald-Giemsa staining

Antigen presenting cells purified from NCD and HFD mice were resuspended in 500 μl PBS containing 50 % FBS and spun down onto a glass slide using a Cytospin centrifuge (Thermo Scientific). The glass slides were incubated with May-Grunwald solution (Wako Pure Chemical Industries) for 5 min, washed with distilled water for 2 min, incubated with 5 %

Giemsa stain solution (Wako Pure Chemical Industries) for 10 min, and mounted.

Statistical analysis

Results are presented as the mean ± S.E.M. Statistical significance was evaluated with an unpaired two-tailed Student's t-test, one-way ANOVA, or two-way ANOVA. Significance was set at $p \leq 0.05$. * $p < 0.05$, ** $p < 0.01$, *** $p < 0.001$

Results

Small intestinal T_H17 cells are reduced in obese mice

To investigate the effects of HFD-induced obesity on the intestinal immune system, we analyzed the distribution of $CD4^+$ T_H subsets in the small intestinal lamina propria (SI LP) of mice fed NCD or HFD for 10 weeks. Using intracellular cytokine staining, we found that the proportion of IL-17^+ T_H17 cells was significantly decreased, with a concomitant increase in IFN-γ^+ T_H1 cells, in SI of HFD mice (Figure 1*A* and *B*). Among IL-17^+ T_H17 cells, the proportion of IL-17^+IL-22^+ cells was also decreased whereas that of IL-17^+GM-CSF^+ cells did not change (Supplementary Figure 1*A* and *B*). A reduction in T_H17 cells was similarly observed in *ob/ob* mice, a genetic model of obesity and type 2 diabetes (data not shown). We confirmed these results by intracellular staining of the master transcription factor for each T_H subset, which showed a reduction of RORγt^+ T_H17 cells and an increase of T-bet^+ T_H1 cells in HFD mice (Figure 1*C*). The percentage of $Foxp3^+$ Treg or GATA-3^+ T_H2 cells was not significantly altered. Neither was the percentage of RORγt^+T-bet^+ or RORγt^+Foxp3^+ T cells (Supplementary Figure 1*C*). In accordance with these opposite changes in the T_H1 and T_H17 cell population, SI $CD4^+$ T cells isolated from HFD mice produced significantly more IFN-γ and less IL-17 and IL-22 than cells isolated from NCD mice (Figure 1*D* and Supplementary Figure 1*D*). The levels of IL-13 and IL-10 were comparable.

Unlike T_H ($CD4^+$ $\alpha\beta$ T) cells, $\gamma\delta$ T cells in SI LP were not affected by HFD (Supplementary Figure 2*A* and *B*). We also analyzed intraepithelial T cells (IEL) in SI and found that the proportion of $\gamma\delta$ TCR^+ IELs was increased over $\alpha\beta$ TCR^+ IELs in HFD mice (Supplementary Figure 2*C* and *D*). In both $\alpha\beta$ TCR^+ and $\gamma\delta$ TCR^+ IELs, HFD increased IFN-γ^+ cells whereas the proportion of IL-17^+ IELs showed little change. Collectively, these data show that HFD induces marked changes in the intestinal T cell population of mice, including

a reduction in T_H17 cells.

Alteration of antigen-presenting cells in the small intestine of HFD mice

Antigen presenting cells (APCs), such as dendritic cells (DCs) and macrophages, modulate T_H cell differentiation through antigen presentation and cytokine production.[23, 24] Therefore, we checked if HFD induces alterations of SI APCs. The low density MHC-II$^+$ cells in SI can be divided into two major populations: CD103$^+$CX3CR1$^-$ DCs (CD103$^+$ DCs) and CD103$^-$CX3CR1$^+$ mononuclear phagocytes (CX3CR1$^+$ cells)[25], which we further divided into CD11c^{hi} (R2) and CD11c^{lo} (R3) subsets (Figure 2*A*). May-Gruwald-Giemsa staining showed that the R2 and R3 subsets possessed many phagocytic vesicles in their cytoplasm, suggesting that they vigorously sample luminal antigens (Figure 2*B*). We were also able to observe the three phenotypically distinguishable APC subsets by immunohistochemistry (Figure 2*C*). The R1 subset showed the highest expression of costimulatory molecules such as CD80 and CD86, whereas the R2 and R3 subsets highly expressed F4/80, CCR2, and CD206, which are often highly expressed in macrophages (Figure 2*D*). A small portion of cells in the R2 and R3 subsets also expressed Ly6C and Ly6G. In T_H differentiation assay, T_H1 cells were highly induced by the R2 subset, whereas the R3 subset was most efficient in inducing T_H17 cells (Figure 2*E* and *F*).

When we compared the APC subset distribution in NCD and HFD mice, we found that HFD did not induce obvious changes in the proportions of CD103$^+$ DCs and CX3CR1$^+$ cells (data not shown). However, among CX3CR1$^+$ cells, CX3CR1$^+$CD11c^{hi} (R2) cells were increased and CX3CR1$^+$CD11c^{lo} (R3) cells were significantly reduced in HFD mice, correlating with the increased T_H1 and decreased T_H17 cells in HFD mice (Figure 2*G*). We also tested if HFD changes the ability of APCs to induce T_H differentiation. We tried to purify each subset from HFD mice, but could not obtain a sufficient number of live

$CX3CR1^{+}CD11c^{lo}$ (R3) cells from HFD mice due to their severe reduction. We thus purified $CD103^{+}$ DCs (R1) and $CX3CR1^{+}$ cells (R2 + R3) from NCD and HFD mice and compared their ability to induce T_H1 and T_H17 differentiation *in vitro*. We found that HFD enhanced $CD103^{+}$ DCs' ability to induce T_H1 differentiation while inhibiting $CX3CR1^{+}$ cells' ability to induce T_H17 differentiation (Figure 2*H* and *I*). Notably, these HFD-induced changes of APC characteristics correlate well with the increased T_H1 cells and reduced T_H17 cells observed in SI of HFD mice. Therefore, the dramatic reduction of the R3 subset, together with the functional alteration of APCs in HFD mice, likely contributes to the decrease of the SI T_H17 population.

A further reduction of SI T_H17 cells in obese mice by vitamin A depletion correlates with deterioration of metabolic disorders

IL-17 inhibits adipogenesis and regulates glucose metabolism in mice.[26] In addition, IL-17 controls intestinal barrier function, disruption of which is linked to development of obesity and insulin resistance.[27, 28] Therefore, we hypothesized that reduction of intestinal T_H17 cells may contribute to HFD-induced metabolic disorders and examined if further reduction of SI T_H17 cells below the level found in HFD mice would worsen the HFD-induced obesity. It was reported that vitamin A depletion from a diet significantly lowers SI T_H17 cell numbers.[29-31] Consistent with these reports, we found that SI T_H17 cells were severely reduced in mice fed vitamin A-depleted HFD (VAD) compared to mice fed vitamin A-sufficient HFD (VAS) (Figure 3*A*). The proportion of T_H1 cells was slightly increased and Treg cells were not affected by VAD. Moreover, mice on VAD gained significantly more weight than the ones fed VAS (Figure 3*B*). The epididymal fat mass was also higher in VAD mice (Figure 3*C*). Furthermore, VAD mice showed significantly higher fasting serum glucose and insulin levels as well as exacerbated glucose intolerance and insulin resistance (Figure

3*D-G*). Obesity induces infiltration of macrophages into VAT and their phenotypic switch from an M2- into an M1-polarized state.[7, 8, 22] We found that the percentage and the number of VAT M2 macrophages were lower in VAD mice (Figure 3*H*). These data suggest that reduction of SI T_H17 cells correlates with the severity of obesity and metabolic disorders and imply that enhancement of SI T_H17 cells in obese mice may show a beneficial effect.

Adoptive transfer of gut-tropic T_H17 cells improves obesity and metabolic syndrome

To see if the restoration of SI T_H17 cells might lessen the weight gain and obesity-associated metabolic syndrome, we directly tested the role of T_H17 cells in HFD mice using an adoptive T cell transfer method. For this, we injected *in vitro* differentiated T_H17 cells into Rag1-deficient mice fed HFD for 10 weeks and monitored the mice for additional 5 weeks with continuous HFD (Figure 4*A*). To ensure efficient targeting of transferred cells to SI, we added 1 nM RA during T_H17 differentiation[32] and verified the expression of CCR9 and $\alpha_4\beta_7$ integrin on T_H17 cells (data not shown). Also, we co-injected the same numbers of purified Treg cells together with T_H17 cells to prevent T_H17-mediated inflammation and used the mice that received Treg alone or PBS as controls. Strikingly, we found that the co-injection of T_H17 and Treg cells reversed the weight gain and decreased the fat mass despite the continuous HFD (Figure 4*B* and *C*). In contrast, transfer of Treg cells alone had no effect. The co-transfer of T_H17/Treg cells also lowered the fasting glucose and insulin levels and improved glucose tolerance and insulin sensitivity (Figure 4*D-G*). The T_H17/Treg-transfer also increased VAT M2 macrophages (Figure 4*H* and *I*). Furthermore, HFD-induced lipid accumulation in the liver was dramatically reversed by the T_H17/Treg-transfer (Figure 4*J*). The mice that received T_H17 cells together with Treg cells displayed no evidence of impaired food intake or intestinal inflammation (Supplementary Figure 3). As a comparison, we also transferred *in vitro* differentiated, gut-tropic T_H1 cells together with Treg cells. Similarly to

T_H17 cells, T_H1 cells were highly enriched in SI, but we did not observe a significant improvement of metabolic disorders in the T_H1/Treg-transferred mice compared to the T_H17/Treg-transferred mice, indicating that the beneficial effect of the T_H cell transfer is specific to T_H17 cells (Supplementary Figure 4*A*-*I*).

Gut-tropic T_H17 cells induce a shift in gut microbiota composition in HFD mice

Alteration of the intestinal T cell population can result in the modification of gut microbiota.[17] Moreover, disturbance of gut microbiota composition, resulting in fewer *Bacteroidetes* and more *Firmicutes* compared to lean controls, is linked to obesity and metabolic syndrome in both mice and humans.[16] Therefore, we performed metagenomic analysis of fecal bacteria in HFD mice before and after the adoptive T cell transfer to determine if the increase in intestinal T_H17 cells changed the composition of gut microbiota. Indeed, the T_H17/Treg co-transfer led to a large shift in the fecal microbiota composition of HFD mice (Figure 5*A*). Specifically, we observed a significant increase of *Bacteroidetes* and a decrease of *Firmicutes* at the phylum level after the T_H17/Treg transfer (Figure 5*B*). Interestingly, similar changes were observed in obese humans who succeeded in weight loss through a low-calorie diet[11], suggesting that SI T_H17 cells may promote an intestinal microenvironment favoring the expansion of commensal microbes associated with leanness. Fecal microbiota in Treg-transferred mice showed a relatively smaller change compared to T_H17/Treg transferred mice, with an increase of *Proteobacteria* and a decrease of *Bacteroidetes*. The difference of fecal microbiota in T_H17/Treg- and Treg-transferred mice was also evident at the family and genus levels. After the T_H17/Treg-transfer, *Lachnospiraceae* and *Heliocobacteraceae* were decreased, whereas *Ruminococcaceae*, *Rikenellaceae*, and *Porphyromonadaceae* were increased (Figure 5*C*). Notably, we observed the opposite changes of these bacteria in Treg-transferred mice. Several genera, including

Helicobacter, *Oscillibacer*, and *Rikenella*, were also inversely changed in T_H17/Treg- and Treg-transferred mice (Figure 5*D*). Recently, a mucin-degrading bacterium *Akkermansia muciniphila* was found to be reduced in obese and type 2 diabetic mice, and treatment with *A. muciniphila* reversed HFD-induced metabolic disorders.[33, 34] Indeed, *Akkermansia* genus bacteria were hardly detected in the feces of HFD mice before the T cell transfer. However, after the T_H17/Treg-transfer, the abundance of *Akkermansia* dramatically increased (Figure 5*D*). We also found an increase of *Akkermansia*, albeit to a less extent, after the Treg-transfer. By using *A. muciniphila*-specific primers, we confirmed our findings in qPCR analysis (Figure 5*E*). In contrast, the T_H1/Treg-transfer did not increase *A. muciniphila* (Supplementary Figure 4*J*). Segmented filamentous bacteria (SFB), belonging to *Lachnospiraceae*, induce intestinal T_H17 cells[35], and intestinal IL-17 signaling reciprocally controls the abundance of SFB.[36] Consistent with these findings, we found the reduction of SFB after the T_H17/Treg-transfer, but not after the Treg- or T_H1/Treg-transfer (Figure 5*F* and Supplementary Figure 4*K*).

To test if the altered gut microbiota in the T_H17/Treg-transferred mice contributes to weight control and glucose homeostasis, we transplanted the fecal bacteria collected from Treg- and T_H17/Treg-transferred HFD mice into lean, wild type mice by oral gavage. The recipient mice were pretreated with antibiotic mixture to reduce endogenous gut microbiota and fed with NCD during the entire experiments. The mice that received the fecal bacteria of T_H17/Treg-transferred HFD mice showed less weight gain, less fat mass, and lower fasting serum glucose levels compared to mice which received the fecal bacteria from Treg-transferred HFD mice (Supplementary Figure 5*A*-*C*). Serum insulin levels and glucose tolerance test did not show significant differences between the two groups, whereas insulin sensitivity seemed slightly better in mice that received the fecal bacteria from T_H17/Treg-transferred mice (Supplementary Figure 5*D*-*F*). These results support a notion that gut-tropic

T_H17 cells promote the expansion of gut microbiota that is beneficial for metabolic homeostasis.

Gut-homing property of the transferred T_H17 cells is critical for improving obesity and metabolic syndrome

To examine if the transferred T_H17 cells indeed migrated to the gut, we analyzed T cells in the recipient mice and found a preferential expansion of T_H17 cells in SI (Figure 6*A* and *B*). Unlike T_H17 cells, only a small number of Treg cells were found in SI. To assess if the gut-homing property of T_H17 cells is important for their beneficial effects, we injected wild type or β7 integrin-deficient T_H17 cells together with Treg cells into HFD mice. As expected, much fewer β7 integrin-deficient T_H17 cells were detected in SI compared to wild type T_H17 cells (Figure 6*C*). Consequently, mice that received β7 integrin-deficient T_H17 cells had more fat mass and bigger adipocytes compared to the ones that received wild type T_H17 cells (Figure 6*D-F*). They also exhibited higher fasting glucose levels (figure 6*G*). Serum insulin levels were similar in both mice, and mice with β7 integrin-deficient T_H17 cells exhibited more severe glucose intolerance and insulin resistance (Figure 6*H-J*). In addition, unlike wild type T_H17 cells, β7 integrin-deficient T_H17 cells failed to reverse the fat accumulation in the liver (Figure 6*K*). Collectively, these data demonstrate that gut homing is necessary for the transferred T_H17 cells to elicit beneficial effects on host metabolism.

Gut-tropic T_H17 cells control obesity and metabolic disorders via IL-17

IL-17 is the major effector cytokine of T_H17 cells. To examine if IL-17 mediates the T_H17-induced restoration of metabolic homeostasis, we compared T_H17 cells prepared from wild type and IL-17-deficient mice in T_H17/Treg co-transfer experiments. Notably, IL-17-

deficient T_H17 cells were not as effective as wild type T_H17 cells in improving obesity and associated metabolic syndrome (Figure 7*A*-*F*). Compared to the transfer of wild type T_H17 cells, the transfer of IL-17-deficient T_H17 cells resulted in less weight loss, more epididymal fat mass, and higher fasting glucose and insulin levels as well as more severe glucose intolerance and insulin resistance. Nonetheless, when compared to mice which received only Treg cells, mice that received IL-17-deficient T_H17 cells showed a significant improvement in weight control and glucose tolerance (Figure 7*A* and *E*). These data indicate that the beneficial effects of gut-tropic T_H17 cells are mainly mediated by IL-17, but additional factors are also involved.

Analysis of gut microbiota revealed that mice having IL-17-deficient T_H17 cells had significantly fewer *Bacteroidetes* and more *Firmicutes* than mice having wild-type T_H17 cells, suggesting that IL-17 is critical for the effects of SI T_H17 cells in promoting expansion of commensal microbes linked with leanness (Figure 7*G*). In the gut, IL-17 enhances protective immunity and regulates commensal bacteria by strengthening epithelial barrier function and inducing antimicrobial peptide production.[37] Paneth cells in the crypts of SI serve as an important source of antimicrobial peptides. In obese humans and mice, antimicrobial peptide production by Paneth cells is significantly reduced.[38] By visualizing Paneth cell granules with *Ulex europaeus* agglutinin (UEA)-1 staining, we observed that mice that received IL-17-deficient T_H17 cells had markedly less granular contents compared to mice which received wild type T_H17 cells (Figure 7*H*). We also found that expression of antimicrobial peptides such as β-defensin3 and Reg3γ was significantly lower in SI of mice that received IL-17-deficient T_H17 cells (Figure 7*I*). These data suggest that intestinal T_H17 cells may regulate obesity-related gut microbiota and host metabolism at least in part by modulating Paneth cell function in an IL-17-dependent manner.

Discussion

HFD causes infiltration of T cells into VAT, which contributes to adipose tissue inflammation and progression of obesity.[1-3] However, a functional role of intestinal T cells in obesity-associated metabolic disorders is not clear.[20] Our current study identified an alteration in SI $CD4^+$ T_H cell proportions, increased T_H1 cells and reduced T_H17 cells, in a 10 week-long HFD-induced obesity model. Despite the reduction of total T_H17 cells, HFD did not change the proportion of GM-CSF^+ or T-bet^+ T_H17 cells, which are considered pathogenic.[39-41] Similarly to our study, Garidou *et al.* reported an increase of T_H1 and a decrease of T_H17 populations in SI of mice fed a short-term (10 or 30 days) HFD, causing early insulin resistance without obesity induction.[18] In contrast, a study by Luck *et al.* reported the expansion of T_H1 cells without a significant change of T_H17 cells in SI after a long-term (12-16 weeks) HFD.[19] Although the exact origin of the discrepancies on the T_H17 alteration is not known at present, they might have derived from several factors, including the composition and duration of HFD, animal housing conditions, resident microbiota, and methods of leukocyte isolation and analysis.[20] A multitude of related mechanisms may underlie the disturbance of $CD4^+$ T_H subset distribution in HFD-induced obese mice. APCs in the intestinal LP uptake antigens across the epithelium and play a crucial role in differentiation of T_H cells.[23] For example, $CX3CR1^+$ cells were reported to mediate the commensal bacteria-induced T_H17 cell differentiation.[42] In this study, we found that HFD induces the alteration of SI APC subset distribution as well as their capacity to induce T_H differentiation. The significant reduction in $CX3CR1^+CD11c^{lo}$ cells, the most efficient T_H17-inducing APC subset, as well as the diminished ability of $CX3CR1^+$ cells to induce T_H17 differentiation in HFD mice could explain, at least partly, the loss of SI T_H17 cells. Future investigation of the effects of gut microbiota dysbiosis and cellular metabolic changes in APCs of HFD mice will likely give some insight on the mechanisms underlying the HFD-induced alteration of APCs.

Gut microbiota is another key factor controlling intestinal immune cells. Dysbiotic gut microbiota was reported to cause a reduction of SI T_H17 cells in non-obese mice with early type 2 diabetes.[18] In comparison, our study demonstrated that reestablishment of SI T_H17 cells by the adoptive transfer in obese mice resulted in restoration of the *lean* gut microbiota by promoting a significant increase of *Bacteroidetes* and a decrease of *Firmicutes*. We also observed differential microbiota changes at the family and genus levels after the T_H17/Treg- and Treg-transfer into HFD mice. Interestingly, the decrease of *Lachnospiraceae* and the increase of *Porphyromonadaceae* and *Sutterellaceae* seen in T_H17/Treg-transferred mice were also observed by Garidou *et al*. in the synbiotic-treated HFD mice showing increased T_H17 cells and improved insulin sensitivity.[18] Moreover, the T_H17/Treg-transfer significantly increased *A. muciniphila*, known to prevent HFD-induced metabolic disorders, and the fecal bacteria from T_H17/Treg-transferred mice conferred a more favorable metabolic status in recipient mice compared to the fecal bacteria from Treg-transferred mice, highlighting the importance of SI T_H17 cells in controlling gut microbiota and alleviating obesity-related metabolic syndrome.

T_H17 cells secrete several cytokines. IL-17-deficient T_H17 cells were much less efficient than wild type cells in improving gut microbiota and metabolic disorders in HFD mice, suggesting that the beneficial effects of gut-tropic T_H17 cells are mainly mediated by IL-17. However, the transfer of IL-17-deficient T_H17 cells still showed a significant improvement in weight gain and glucose tolerance in HFD mice compared to the Treg transfer. Therefore, further assessment of the roles of other T_H17 effector cytokines would seem necessary for full understanding of how SI T_H17 cells regulate intestinal microbiota and the host metabolism. Of note, we found that HFD decreased IL-22 production in SI T_H17 cells, a cytokine shown to alleviate metabolic disorders.[43] Additionally, SI T_H17 cells can transdifferentiate into IL-10-producing Tr1 cells under inflammatory conditions.[44] SI T_H17

cells also promote production of IgA[45], which may potentially contribute to the regulation of systemic insulin resistance via IgA-mediated modulation of microbiota composition.

The decrease of T_H17 cells and IL-17 observed in SI of HFD mice is not ubiquitous. In fact, elevated levels of IL-17 were observed in peripheral blood, adipose tissues and livers of obese subjects[46-49], and obesity-dependent expansion of T_H17 cells was associated with inflammatory autoimmune diseases in brain and colon.[50] Similarly, IL-17^+ mucosal-associated invariant T cells were increased in blood and adipose tissues of obese patients.[51] These results suggest that the functions of SI T_H17 cells are unique, controlling intestinal barriers and commensal microbiota, and distinct from T_H17 cells which become elevated by inflammatory stimuli in the other organs having few IL-17-producing cells in steady state. Moreover, effective improvement of metabolic syndrome by the T_H17 transfer in obese mice required β7 integrin and gut homing of T_H17 cells. Therefore, for a therapeutic application, it would be crucial to achieve gut-specific delivery of T_H17 cells, avoiding systemic side effects of T_H17 cells and their effector cytokines.

REFERENCES

1. Odegaard JI, Chawla A. The immune system as a sensor of the metabolic state. Immunity 2013;38:644-654.
2. Kanneganti TD, Dixit VD. Immunological complications of obesity. Nat Immunol 2012;13:707-712.
3. Osborn O, Olefsky JM. The cellular and signaling networks linking the immune system and metabolism in disease. Nat Med 2012;18:363-374.
4. **Winer S**, **Chan Y**, Paltser G, et al. Normalization of obesity-associated insulin resistance through immunotherapy. Nat Med 2009;15:921-929.
5. Nishimura S, Manabe I, Nagasaki M, et al. CD8+ effector T cells contribute to macrophage recruitment and adipose tissue inflammation in obesity. Nat Med 2009;15:914-920.
6. Wu D, Molofsky AB, Liang HE, et al. Eosinophils sustain adipose alternatively activated macrophages associated with glucose homeostasis. Science 2011;332:243-247.
7. Weisberg SP, McCann D, Desai M, et al. Obesity is associated with macrophage accumulation in adipose tissue. J Clin Invest 2003;112:1796-1808.
8. Lumeng CN, Bodzin JL, Saltiel AR. Obesity induces a phenotypic switch in adipose tissue macrophage polarization. J Clin Invest 2007;117:175-184.
9. **Shin NR**, **Lee JC**, **Lee HY**, et al. An increase in the Akkermansia spp. population induced by metformin treatment improves glucose homeostasis in diet-induced obese mice. Gut 2014;63:727-735.
10. **Schulz MD**, **Atay C**, Heringer J, et al. High-fat-diet-mediated dysbiosis promotes intestinal carcinogenesis independently of obesity. Nature 2014;514:508-512.
11. Ley RE, Turnbaugh PJ, Klein S, et al. Microbial ecology: human gut microbes associated with obesity. Nature 2006;444:1022-1023.
12. Tremaroli V, Backhed F. Functional interactions between the gut microbiota and host metabolism. Nature 2012;489:242-249.
13. Perry RJ, Peng L, Barry NA, et al. Acetate mediates a microbiome-brain-beta-cell axis to promote metabolic syndrome. Nature 2016;534:213-217.
14. Turnbaugh PJ, Backhed F, Fulton L, et al. Diet-induced obesity is linked to marked but reversible alterations in the mouse distal gut microbiome. Cell Host Microbe

2008;3:213-223.

15. **Rabot S**, **Membrez M**, Bruneau A, et al. Germ-free C57BL/6J mice are resistant to high-fat-diet-induced insulin resistance and have altered cholesterol metabolism. FASEB J 2010;24:4948-4959.
16. Turnbaugh PJ, Ley RE, Mahowald MA, et al. An obesity-associated gut microbiome with increased capacity for energy harvest. Nature 2006;444:1027-1031.
17. Hooper LV, Littman DR, Macpherson AJ. Interactions between the microbiota and the immune system. Science 2012;336:1268-1273.
18. **Garidou L**, **Pomie C**, Klopp P, et al. The Gut Microbiota Regulates Intestinal CD4 T Cells Expressing RORgammat and Controls Metabolic Disease. Cell Metab 2015;22:100-112.
19. **Luck H**, **Tsai S**, Chung J, et al. Regulation of obesity-related insulin resistance with gut anti-inflammatory agents. Cell Metab 2015;21:527-542.
20. Winer DA, Luck H, Tsai S, et al. The Intestinal Immune System in Obesity and Insulin Resistance. Cell Metab 2016;23:413-426.
21. **Jang MH**, **Sougawa N**, Tanaka T, et al. CCR7 is critically important for migration of dendritic cells in intestinal lamina propria to mesenteric lymph nodes. J Immunol 2006;176:803-810.
22. **Hong CP**, **Yun CH**, Lee GW, et al. TLR9 regulates adipose tissue inflammation and obesity-related metabolic disorders. Obesity (Silver Spring) 2015;23:2199-2206.
23. Denning TL, Wang YC, Patel SR, et al. Lamina propria macrophages and dendritic cells differentially induce regulatory and interleukin 17-producing T cell responses. Nat Immunol 2007;8:1086-1094.
24. **Uematsu S**, **Fujimoto K**, Jang MH, et al. Regulation of humoral and cellular gut immunity by lamina propria dendritic cells expressing Toll-like receptor 5. Nat Immunol 2008;9:769-776.
25. **Schulz O**, **Jaensson E**, Persson EK, et al. Intestinal CD103+, but not CX3CR1+, antigen sampling cells migrate in lymph and serve classical dendritic cell functions. J Exp Med 2009;206:3101-3114.
26. Zuniga LA, Shen WJ, Joyce-Shaikh B, et al. IL-17 regulates adipogenesis, glucose homeostasis, and obesity. J Immunol 2010;185:6947-6959.
27. **Lee JS**, **Tato CM**, Joyce-Shaikh B, et al. Interleukin-23-Independent IL-17 Production Regulates Intestinal Epithelial Permeability. Immunity 2015;43:727-738.

28. **Cani PD**, **Amar J**, **Iglesias MA**, et al. Metabolic endotoxemia initiates obesity and insulin resistance. Diabetes 2007;56:1761-1772.

29. Hall JA, Cannons JL, Grainger JR, et al. Essential role for retinoic acid in the promotion of CD4(+) T cell effector responses via retinoic acid receptor alpha. Immunity 2011;34:435-447.

30. **Cha HR**, **Chang SY**, Chang JH, et al. Downregulation of Th17 cells in the small intestine by disruption of gut flora in the absence of retinoic acid. J Immunol 2010;184:6799-6806.

31. Kang SG, Wang C, Matsumoto S, et al. High and low vitamin A therapies induce distinct FoxP3+ T-cell subsets and effectively control intestinal inflammation. Gastroenterology 2009;137:1391-1402 e1-6.

32. Wang C, Kang SG, HogenEsch H, et al. Retinoic acid determines the precise tissue tropism of inflammatory Th17 cells in the intestine. J Immunol 2010;184:5519-5526.

33. Everard A, Belzer C, Geurts L, et al. Cross-talk between Akkermansia muciniphila and intestinal epithelium controls diet-induced obesity. Proc Natl Acad Sci U S A 2013;110:9066-9071.

34. Plovier H, Everard A, Druart C, et al. A purified membrane protein from Akkermansia muciniphila or the pasteurized bacterium improves metabolism in obese and diabetic mice. Nat Med 2017;23:107-113.

35. **Ivanov, II**, **Atarashi K**, Manel N, et al. Induction of intestinal Th17 cells by segmented filamentous bacteria. Cell 2009;139:485-498.

36. Kumar P, Monin L, Castillo P, et al. Intestinal Interleukin-17 Receptor Signaling Mediates Reciprocal Control of the Gut Microbiota and Autoimmune Inflammation. Immunity 2016;44:659-671.

37. Ishigame H, Kakuta S, Nagai T, et al. Differential roles of interleukin-17A and -17F in host defense against mucoepithelial bacterial infection and allergic responses. Immunity 2009;30:108-119.

38. Hodin CM, Verdam FJ, Grootjans J, et al. Reduced Paneth cell antimicrobial protein levels correlate with activation of the unfolded protein response in the gut of obese individuals. J Pathol 2011;225:276-284.

39. **Codarri L**, **Gyulveszi G**, Tosevski V, et al. RORgammat drives production of the cytokine GM-CSF in helper T cells, which is essential for the effector phase of autoimmune neuroinflammation. Nat Immunol 2011;12:560-567.

40. **El-Behi M**, **Ciric B**, Dai H, et al. The encephalitogenicity of T(H)17 cells is dependent on IL-1- and IL-23-induced production of the cytokine GM-CSF. Nat Immunol 2011;12:568-575.
41. Yang Y, Weiner J, Liu Y, et al. T-bet is essential for encephalitogenicity of both Th1 and Th17 cells. J Exp Med 2009;206:1549-1564.
42. Panea C, Farkas AM, Goto Y, et al. Intestinal Monocyte-Derived Macrophages Control Commensal-Specific Th17 Responses. Cell Rep 2015;12:1314-1324.
43. **Wang X**, **Ota N**, Manzanillo P, et al. Interleukin-22 alleviates metabolic disorders and restores mucosal immunity in diabetes. Nature 2014;514:237-241.
44. Gagliani N, Vesely MC, Iseppon A, et al. Th17 cells transdifferentiate into regulatory T cells during resolution of inflammation. Nature 2015;523:221-225.
45. Cao AT, Yao S, Gong B, et al. Th17 cells upregulate polymeric Ig receptor and intestinal IgA and contribute to intestinal homeostasis. J Immunol 2012;189:4666-4673.
46. **Sumarac-Dumanovic M**, **Stevanovic D**, Ljubic A, et al. Increased activity of interleukin-23/interleukin-17 proinflammatory axis in obese women. Int J Obes (Lond) 2009;33:151-156.
47. **Fabbrini E**, **Cella M**, McCartney SA, et al. Association between specific adipose tissue CD4+ T-cell populations and insulin resistance in obese individuals. Gastroenterology 2013;145:366-374 e1-3.
48. Pandolfi JB, Ferraro AA, Sananez I, et al. ATP-Induced Inflammation Drives Tissue-Resident Th17 Cells in Metabolically Unhealthy Obesity. J Immunol 2016;196:3287-3296.
49. Chackelevicius CM, Gambaro SE, Tiribelli C, et al. Th17 involvement in nonalcoholic fatty liver disease progression to non-alcoholic steatohepatitis. World J Gastroenterol 2016;22:9096-9103.
50. **Winer S**, **Paltser G**, Chan Y, et al. Obesity predisposes to Th17 bias. Eur J Immunol 2009;39:2629-2635.
51. **Magalhaes I**, **Pingris K**, Poitou C, et al. Mucosal-associated invariant T cell alterations in obese and type 2 diabetic patients. J Clin Invest 2015;125:1752-1762.

Author names in bold designate shared co-first authorship.

Figure legends

Figure 1 HFD results in a decrease of SI T_H17 cells. (A) Intracellular IFN-γ and IL-17 expression profile of TCRβ$^+$CD4$^+$ T cells in spleen (SP), mesenteric lymph nodes (MLN), visceral adipose tissue (VAT), and small intestine (SI) (B) Proportion of T_H1 (IFN-γ$^+$) cells and T_H17 (IL-17$^+$) cells. Box inserted in the bottom graph shows the proportion of MLN T_H17 cells. Dot plots show pooled data from five independent experiments (SP, MLN: n=12~13; VAT, SI: n=17~22). (C) Proportion of T-bet$^+$, RORγt$^+$, GATA3$^+$ and Foxp3$^+$ TCRβ$^+$CD4$^+$ T cells in SI (n=6 per group). (D) Cytokine secretion by TCRβ$^+$CD4$^+$ T cells purified from SI was measured using ELISA after stimulation with anti-CD3 and anti-CD28 antibodies for 24 h.

Figure 2 HFD induces alteration of SI APCs. (A) The low density MHC-II$^+$ cells in SI of NCD mice were divided into three subsets based on CD103, CX3CR1, and CD11c expression. (B) May-Grunwald-Giemsa staining of APC subsets. Original magnification, 1000 x. (C) Immunochemistry of CX3CR1 (green) and CD11c (red) cells in SI from CX3CR1-GFP mice. Scale bars, 50 μm. (D) Surface marker expression in APC subsets. Shaded histograms represent isotype controls. (E and F) Naïve OT-II T cells were co-cultured with APC subsets in the presence of OVA peptide alone (E) or together with TGFβ and IL-6 (F). The proportion of T_H1 and T_H17 cells were measured by intracellular cytokine staining. (G) The proportion of R1, R2, and R3 cells in SI of NCD and HFD mice (n=7 per group). (H) Naïve OT-II T cells were co-cultured with CD103$^+$ DCs or CX3CR1$^+$ cells purified from NCD and HFD mice. The proportion of T_H1 and T_H17 cells were measured by intracellular cytokine staining. (I) T cells cultured as in (H) were stimulated with anti-CD3 and anti-CD28 antibodies and production of IFN- γ and IL-17 was measured by ELISA.

Figure 3 Downregulation of SI T_H17 cells via vitamin A depletion aggravates obesity and metabolic disorders. (A) Proportion of T_H cells in VAS and VAD mice (n=7 per group). (B) Body weight gain. (C) Epididymal fat mass. Scale bar: 1 cm. (D) Fasting serum glucose level. (E) Fasting serum insulin level. (F) Glucose tolerance test. (G) Insulin tolerance test. (H) Flow cytometry analysis of macrophages ($CD11b^+MHCII^+F4/80^+$) in VAT. The proportion of M2 ($CD206^{hi}$) macrophages were analyzed.

Figure 4 Adoptive transfer of gut-tropic T_H17 cells improves obesity and metabolic syndrome. (A) Experimental scheme (n=4-8 per group). (B) Body weight changes after the T cell transfer. (C) Epididymal fat mass. Scale bar: 1 cm. (D) Fasting serum glucose level. (E) Fasting serum insulin level. (F) Glucose tolerance test. (G) Insulin tolerance test. (H) Flow cytometric analysis of macrophages in VAT. (I) Proportion and numbers of M2 ($CD206^+$) macrophages in VAT. (J) Oil-red O staining of the liver. Original magnification, 400 x.

Figure 5 Adoptive transfer of T_H17 and Treg cells induces alteration of gut microbiota. Fecal samples were collected from the recipient mice one day before and 5 weeks after the T cell transfer and analyzed for the microbiota composition. (A) Principle coordinate analysis. (B-D) Taxonomic comparison at the phylum (B), family (C) and genus (D) levels. (E and F) Relative abundance of *A. muciniphila* (E) and *SFB* (F) was analyzed by qPCR (n=5 per group)

Figure 6 T_H17 cells lacking β7 integrin fail to improve obesity and metabolic syndrome. (A and B) HFD Rag1-null mice were injected with a combination of $5x10^5$ Treg cells and $5x10^5$ T_H17 ($Thy1.1^+$) cells (n=5 per group). (A) Proportion of T_H17 ($Thy1.1^+$) and Treg ($Foxp3^+$) cells in SP and SI at 72 h and at 4 weeks after the transfer. (B) Proportion and total number of

T_H17 and Treg cells. (C-K) HFD Rag1-null mice were injected with Treg and T_H17 (WT or β7 integrin-deficient) cells and remained on a HFD for additional 5 weeks (n=4 per group). (C) Proportion of T_H17 cells in SI at 5 weeks after the transfer. (D) Body weight changes. (E) Epididymal fat mass. Scale bar: 1 cm. (F) Hematoxylin and eosin staining of VAT. Original magnification, 100 x. (G) Fasting serum glucose level. (H) Fasting serum insulin level. (I) Glucose tolerance test. (J) Insulin tolerance test. (K) Oil-red O staining of the liver. Original magnification, 400 x.

Figure 7 IL-17-deficient T_H17 cells fail to improve obesity and glucose homeostasis. HFD Rag1-null mice were injected with Treg and T_H17 (WT or IL-17-deficient) cells and remained on a HFD for additional 5 weeks (n=5 per group). (A) Body weight changes. (B) Epididymal fat mass. Scale bar: 1 cm. (C) Fasting serum glucose level. (D) Fasting serum insulin level. (E) Glucose tolerance test. (F) Insulin tolerance test. (G) qPCR analysis of fecal bacteria in recipient mice after the T cell transfer. Bact, bacteroidetes; Firm, firmicutes; Prot, γ-proteobacteria; Acti, actinobacteria. (H) Confocal image of UEA-1^+ (red) granules in the Paneth cells. Nuclei were stained with DAPI (blue). Scale bar: 20 μm (left), 10 μm (right). (I) qPCR analysis of antimicrobial peptides in the SI of recipient mice.

Figure 1

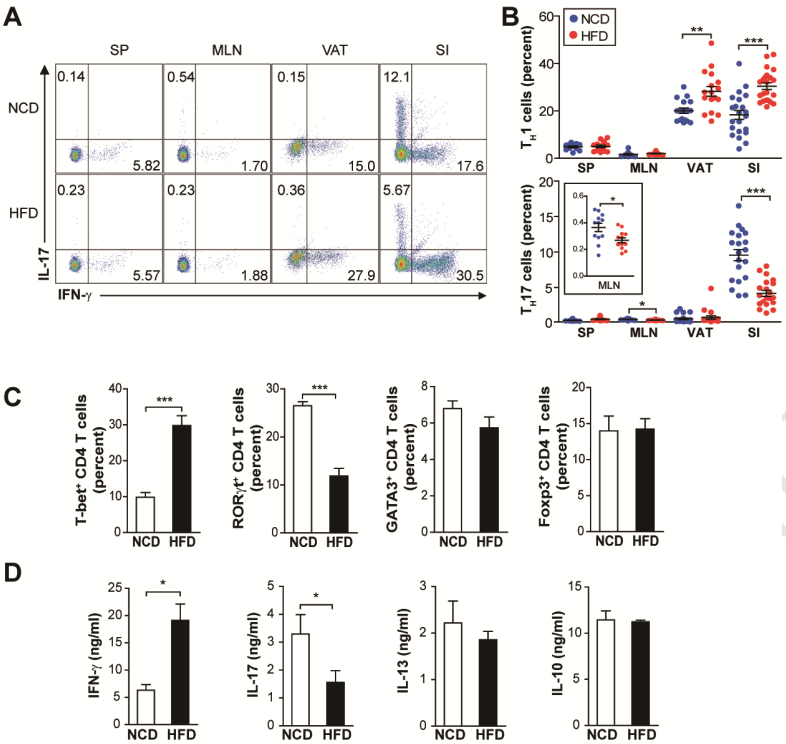

Figure 2

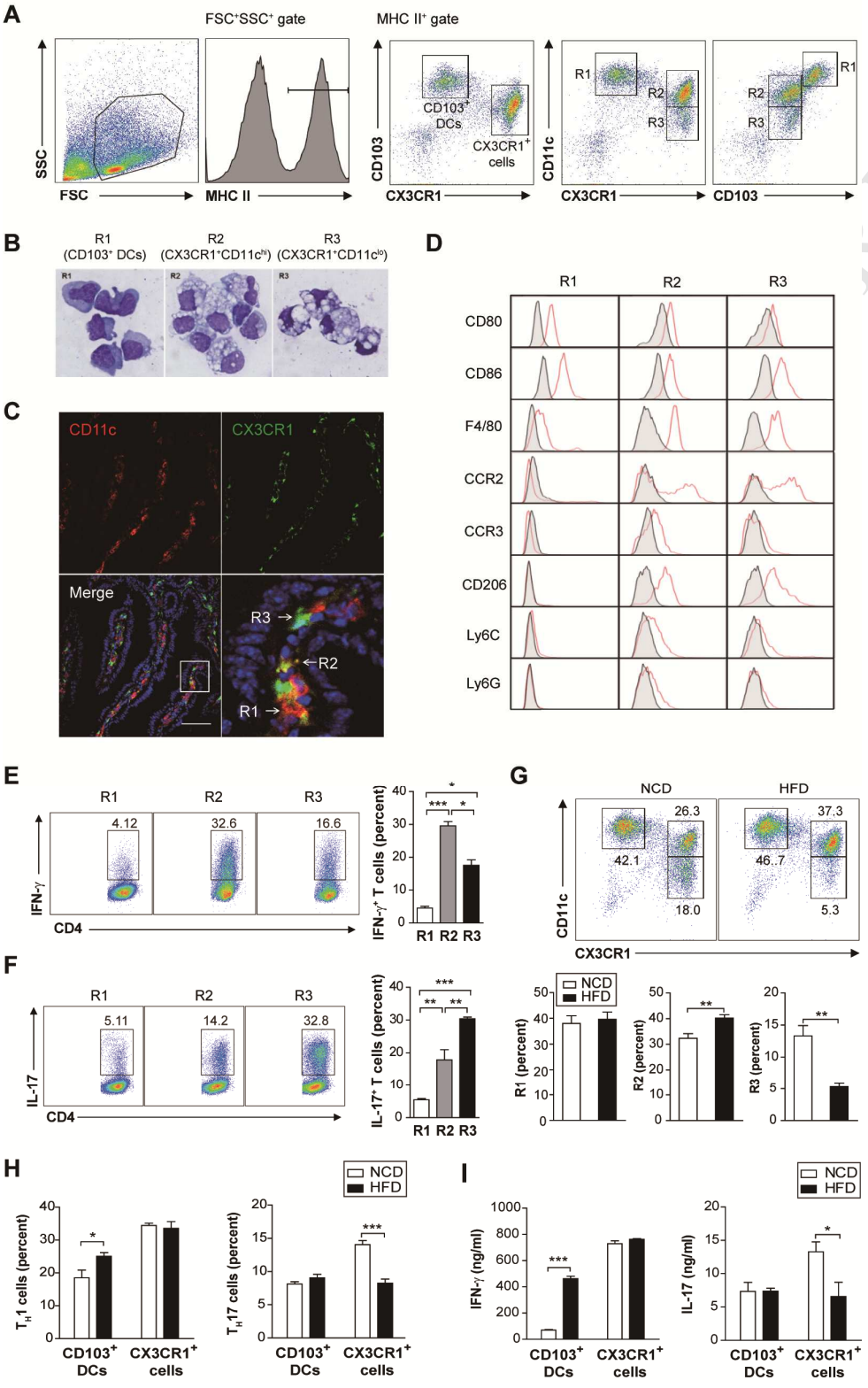
A
FSC+SSC+ gate
MHC II+ gate
SSC
FSC
MHC II
CD103
CX3CR1
CD103+ DCs
CX3CR1+ cells
CD11c
R1
R2
R3
B
R1 (CD103+ DCs)
R2 (CX3CR1+CD11chi)
R3 (CX3CR1+CD11clo)
C
CD11c
CX3CR1
Merge
R3
R2
R1
D
R1
R2
R3
CD80
CD86
F4/80
CCR2
CCR3
CD206
Ly6C
Ly6G
E
R1
R2
R3
4.12
32.6
16.6
IFN-γ
CD4
IFN-γ+ T cells (percent)
R1 R2 R3
F
5.11
14.2
32.8
IL-17
CD4
IL-17+ T cells (percent)
R1 R2 R3
G
NCD
HFD
26.3
37.3
42.1
46..7
18.0
5.3
CD11c
CX3CR1
R1 (percent)
R2 (percent)
R3 (percent)
H
NCD
HFD
TH1 cells (percent)
TH17 cells (percent)
CD103+ DCs
CX3CR1+ cells
I
NCD
HFD
IFN-γ (ng/ml)
IL-17 (ng/ml)
CD103+ DCs
CX3CR1+ cells

Figure 3

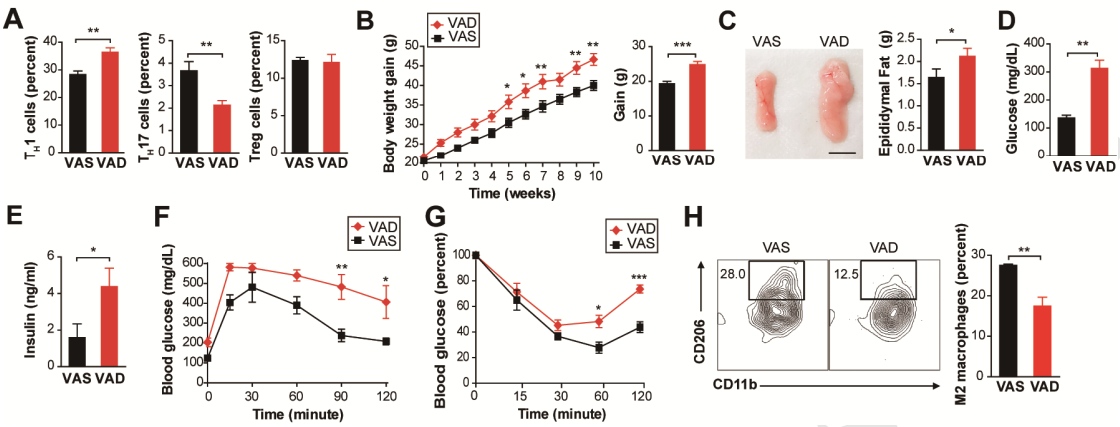

Figure 4

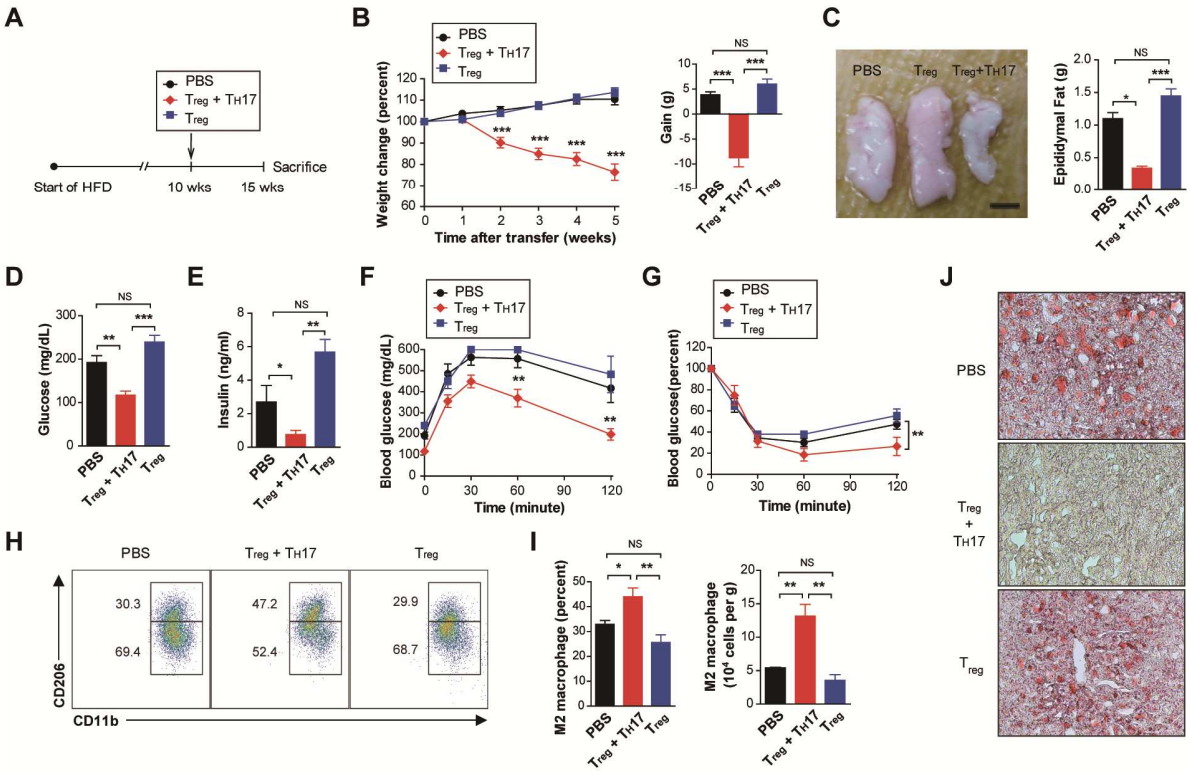

Figure 5

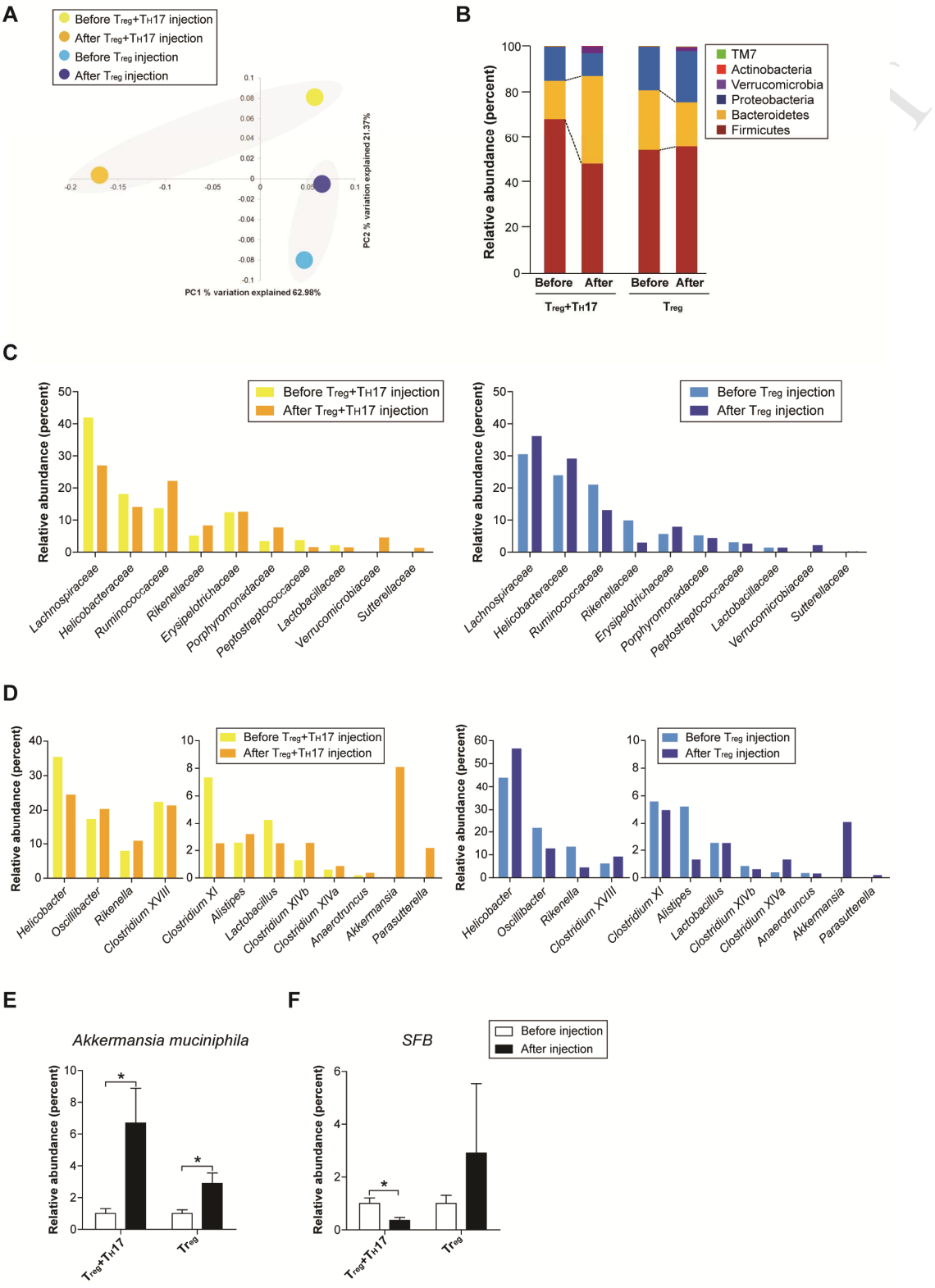
A
Before Treg+TH17 injection
After Treg+TH17 injection
Before Treg injection
After Treg injection
PC1 % variation explained 62.98%
PC2 % variation explained 21.37%
B
Relative abundance (percent)
TM7
Actinobacteria
Verrucomicrobia
Proteobacteria
Bacteroidetes
Firmicutes
Before After Before After
Treg+TH17 Treg
C
Relative abundance (percent)
Before Treg+TH17 injection
After Treg+TH17 injection
Before Treg injection
After Treg injection
Lachnospiraceae
Helicobacteraceae
Ruminococcaceae
Rikenellaceae
Erysipelotrichaceae
Porphyromonadaceae
Peptostreptococcaceae
Lactobacillaceae
Verrucomicrobiaceae
Sutterellaceae
D
Relative abundance (percent)
Before Treg+TH17 injection
After Treg+TH17 injection
Before Treg injection
After Treg injection
Helicobacter
Oscillibacter
Rikenella
Clostridium XVIII
Clostridium XI
Alistipes
Lactobacillus
Clostridium XIVb
Clostridium XIVa
Anaerotruncus
Akkermansia
Parasutterella
E
Akkermansia muciniphila
Relative abundance (percent)
Treg+TH17
Treg
F
SFB
Before injection
After injection
Relative abundance (percent)
Treg+TH17
Treg

Figure 6

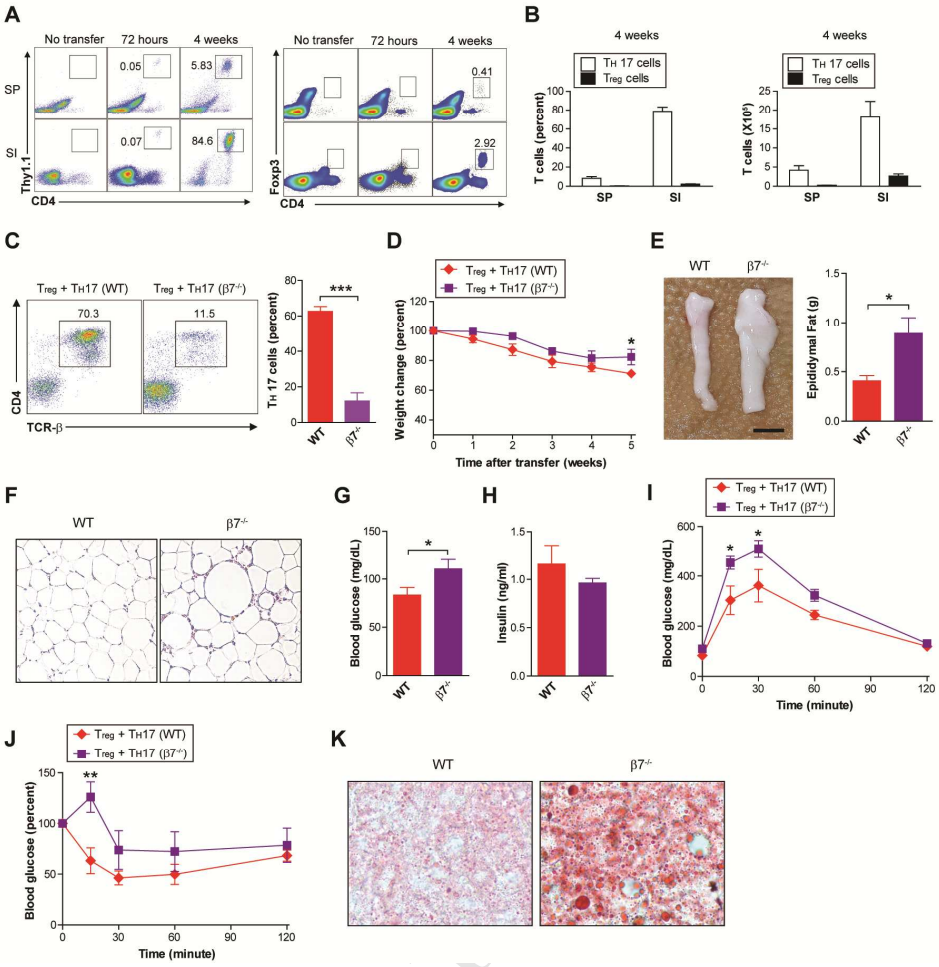

Figure 7